AN IMAGING GAS SCINTILLATION PROPORTIONAL COUNTER FOR THE DETECTION OF SUBKILOELECTRON-VOLT X-RAYS

Charles J. Hailey, William H.-M. Ku, and Michael H. Vartanian

Columbia Astrophysics Laboratory, Columbia University

ABSTRACT

A large area imaging gas scintillation proportional counter (IGSPC) has been constructed for use in X-ray astronomy. The IGSPC consists of a gas scintillation proportional counter (GSPC) with a 1 μm polypropylene window coupled to a multiwire proportional counter (MWPC) via a calcium fluoride window. The MWPC, filled with a mixture of argon, methane, and tetrakis (dimethylamino) ethylene, detects the UV photons emitted by the xenon gas in the GSPC. Over a sensitive area of 21 cm^2 the instrument has a measured energy resolution of 17.5% (FWHM) and 1.9 mm (FWHM) spatial resolution at 1.5 keV.

I. INTRODUCTION

Recent research into gas scintillation proportional counters by ourselves (Anderson et al. 1978; Ku et al. 1979; Hamilton et al. 1980) and others (Charpak, Policarpo, and Sauli 1980; Andresen et al 1978; Hoan et al. 1980; Peacock et al. 1980; Manzo et al. 1980), has demonstrated the enormous versatility of this device for X-ray detection. These counters offer a factor of 2 improvement in energy resolution over conventional proportional counters in the energy range 0.1 to 60 keV (Ku et al. 1979; Hamilton et al. 1980]. The use of a photomultiplier tube array to collect the UV light from the GSPC has demonstrated the feasibility of achieving millimeter resolution imaging capabilities (Hamilton et al. 1980; Charpak, Policarpo, and Sauli 1980; Andresen et al. 1978; Hoan et al. 1980]. Finally, the well defined pulse shape corresponding to X-ray capture in the GSPC allows rise-time discrimination, enhancing the usefulness of this instrument in high background environments such as outer space (Ku et al. 1979, Manzo et al. 1980).

Three years ago, Policarpo (1978) suggested using a photoionization chamber in place of a photomultiplier tube to detect the UV radiation. TEA was found to be a suitable gas for krypton scintillation (Policarpo 1978; Charpak, Policarpo, and Sauli 1980) but a more versatile gas (TMAE) was suggested by Anderson (1981). We extended the usefulness of the GSPC by combining the good energy resolution capabilities of the GSPC with the good spatial resolution capabilities of the MWPC (Ku and Hailey 1981). That instrument, with its 100 μm aluminum foil window, was useful above several kilovolts. We have extended the spectral range of our instrument to the subkiloelectron-volt

X-ray region. We discuss the design and operation of the IGSPC and present data acquired with our counter.

II. INSTRUMENT

The instrument we have designed is shown in Figure 1. The GSPC is a pillbox-shaped chamber of 150-mm diameter. It is made of a machineable ceramic material (Macor). X-rays enter the counter through a polypropylene window. The polypropylene is coated with approximately 100 Å of aluminum to ensure that the window is an electrical ground. The GSPC is designed with an O-ring seal so that the X-ray window may be replaced. The X-ray photons are absorbed by xenon atoms in the drift region. Photoelectrons ejected from the xenon atoms drift to a light producing region defined by two stainless steel meshes held at high voltage. The electrons are accelerated, producing UV photons by excimer deexcitation. The UV photons escape through the calcium fluoride window into the 30 cm × 30 cm × 5 cm MWPC. The MWPC is filled with TMAE and P-20. TMAE moleculres absorb a large fraction of the UV photons. Photoelectrons ejected from the TMAE molecules drift down through a low field region defined by a stainless steel mesh located on the lower surface of the calcium fluoride window and a cathode wire plane located below the window. The photoelectrons are accelerated through the cathode plane toward a high voltage anode plane. A lower cathode plane with wires set orthogonal to the wires on the upper cathode plane defines the total active region. The avalanching electrons are collected on the anode while ions collect on the cathode wires. The charge signals induced on the two cathode planes set perpendicularly to one another are processed digitally to yield the centroid of the charge distribution in orthogonal directions (Reid et al. 1979). Energy information is obtained by collecting the electrons in a charge-sensitive preamplifier attached to the anode plane. Important parameters of the IGSPC are summarized in Table 1.

III. DESIGN

The goal was to build a soft X-ray IGSPC with 18% (FWHM) energy resolution and 1.0 mm (FWHM) spatial resolution at 1 keV. Good energy resolution requires maximizing UV light output from the GSPC and detection by the MWPC. Good UV light production is obtained by using as high a differential voltage as possible on the GSPC without allowing charge multiplication. The UV photons produced are proportional to the thickness of the light producing region so this must be large (Conde, Ferreira, and Ferreira 1977). Good UV collection requires transparent UV window and grids and a large solid angle of interception. The calcium fluoride disk is made as thin as mechanical constraints allow and provides approximately 80% transmission. Optimal position resolution sets additional constraints on design (Ku and Hailey 1981). A flashless getter in a separate chamber connected by two tubes to the main counter chamber maintains the purity of the xenon gas. The upper O-ring seal in the GSPC allows easy replacement of thin windows which are mounted on aluminum carrier plates. The entire GSPC assembly is attached to the MWPC via an O-ring and may be removed to provide access to the MWPC chamber.

IV. MEASURED PERFORMANCE OF THE IGSPC

a. Gain and Energy Resolution

The GSPC was filled with 760 torr of high purity (99.995%) xenon gas. The MWPC was filled with 620 torr of P-20 and 0.3 torr of TMAE. Results similar to those described below were also obtained with an MWPC fill of 608 torr of argon, 152 torr of isobutane, and 0.3 torr of TMAE. A small ^{55}Fe source (5.9 keV Mn-K) was epoxied to a window support rib to allow continual monitoring of gain while measurements were taken at lower energies with a variety of fluorescence X-ray sources. GSPC settings of 0.5 kV and 3.8 kV on the upper and lower grids, respectively, and 0.5 kV on the MWPC cathode were chosen as nominal. Figure 2 shows a typical energy resolution versus anode high voltage curve at 0.94 keV (Cu-L). The curve exhibits a minimum at about 2.2 kV, which was chosen as the nominal anode operating voltage. Figure 2 also shows the total cathode plane output as a function of MWPC anode HV. The system gain tends to run away above about 2.3 kV. Figure 3 summarizes the best energy resolution performance of the IGSPC at the energies measured: 0.28 keV (C-K), 0.68 keV (F-K), 0.94 keV (Cu-L), 1.5 keV (Al-K), 2.3 keV (S-K), 5.9 keV (Mn-K). The results agree well with the expected $E^{-1/2}$ scaling. The 8.5% (FWHM) resolution obtained at 5.9 keV is consistent with energy resolution measurements taken on a photomultiplier tube using the same polypropylene window. The gain of the counter was measured as a function of position. The gain is uniform to better than 10% across the entire 51-mm diameter of the X-ray entrance window. The good gain uniformity is a result of the small X-ray window diameter with respect to the total GSPC diameter (ensuring minimal field fringing at the window edge) as well as the large area of the MWPC which ensures efficient UV collection even for events near the edge of the window. Figure 4 shows the energy resolution as a function of position in the direction parallel to the anode wire direction. The energy resolution is uniform across the entire window as expected from the good gain uniformity. Similar results are obtained in the orthogonal direction.

b. Position Resolution and Sensitivity

We have mapped the counter response over the entire 51-mm polypropylene window. Figure 5 shows a plot of the weighted average position versus the source position parallel to the anode wire direction. Again, similar results were obtained for the direction perpendicular to the anode wire direction. The measurements were taken at 0.94 keV (Cu-L) with a copper anode Henke tube mounted approximately 300 cm from the window plane of the counter and connected via a vacuum vessel to the test chamber. Movable slits defined a 150 μm × 150 μm beam size. The counter response is linear over almost the entire range, slowly flattening towards the window edges. This flattening is due to the loss of light intercepted by the 130 mm x 130 mm MWPC as the X-ray source is displaced from the center. The effect is quite small, in marked contrast to results we had previously obtained with a 75 mm x 75 mm MWPC (Ku and Hailey 1981). The desire to improve our position sensitivity was a prime motivation in going to a larger sized MWPC. Figure 6 shows position-resolution data obtained at different X-ray energies. Various collimation schemes allowed us to obtain measurements at 5.9 keV (Mn-K), 1.5 keV (Al-K), and 0.29 keV (C-K), in addition to our measurement at 0.94 keV (Cu-L). The data have been corrected for the effects of finite source size. The data scales roughly as $E^{-1/2}$. Figure 4 shows the position resolution versus source position parallel to the anode wires. As with the energy resolution, good uniformity is obtained (in both directions).

c. Rise-Time and Background-Rejection Efficiency:

Pulse-shape discrimination has been applied with good success in GSPCs to reject non-X-ray background events (Andresen et al. 1977). The time between initiation of secondary light multiplication and the complete collection of all the light is a function of the electron cloud size, the drift velocity in the absorption region, the size of the scintillation region, and the drift velocity in the scintillation region. For our counter geometry and xenon, this rise time is 2.1 microseconds for X-rays captured near the window. The spread in the rise time is a function of the variance on the size of the electron cloud as it enters the scintillation region, variations in drift velocities arising from distortions in the electric fields, and variations in the depth at which the X-rays are absorbed. These variations can be minimized by maximizing the drift velocity and minimizing the field distortions. The parallel grid geometry of our present counter is ideal for the formation of X-ray pulses. The spread in rise times is less than 0.06 microseconds (1 σ). The rise time is essentially the same for all X-rays in the energy range 0.1 to 6 keV within the central 51-mm active area of the counter, although the spread in rise times increases for lower energy X-rays due to the stronger effect of poor fields near the polypropylene window. The pulse formation times for minimum ionizing particles and γ-rays is much less well-defined and ranges from very short times for those events absorbed in the scintillation region to very long times for those events which track through the whole counter. The narrowness of the rise-time distribution for X-rays then, allows us to set a very narrow rise-time window for acceptance and reject a large percentage of the non-X-ray background events. Background rejection rates of 95% have been achieved while maintaining 90% X-ray acceptance rates. Moreover, more than half of the cosmic ray induced background events occur near the edge of the GSPC and can be rejected by virtue of their location outside the central 51-mm field of view.

V. CONCLUSION

The preliminary results from our soft X-ray IGSPC demonstrate the potential usefulness of this instrument. However, there are several steps we will take to improve the energy and position resolution. Improvement of our gettering system should lead to purer xenon gas and thus larger UV light output. Reducing the calcium fluoride thickness through the use of double pumping and reducing the distance from the lower GSPC grid to the calcium fluoride window should allow better UV collection efficiency and also lessen the intrinsic light cloud spread. Finally, a systematic program to examine various fill gases for our IGSPC will be undertaken. These steps should help us attain our goal of 18% (FWHM) energy resolution and 1.0 mm (FWHM) spatial resolution at 1 keV.

The authors wish to acknowledge helpful discussions with R. Novick. This work was supported by the National Aeronautics and Space Administration under grant NGR 33-008-102. This is Columbia Astrophysics Laboratory Contribution No. 214.

TABLE 1

Parameters of IGSPC's Design

Parameter	IGSPC
GSPC	
- Gas mixture*	xenon
- Gas pressure (torr)*	760
- Absorption depth (mm)	10
- Light multiplication depth (mm)	11
- Bottom grid to UV window (mm)	4
- UV window material	CaF_2
- UV window dimensions (mm)	7.0 x 150
- X-ray window material (μm)	1 polypropylene
- X-ray window dimension (mm)	51 dia.
- Grid transparency	90%
- Nominal HV (kV)*V_3, V_1, V_2	0, 0.5, 4.0
IPC	
- Gas mixture*	TMAE + P-20
- Gas pressure (torr)*	0.3 + 620
- Absorption depth (mm)*	12
- Anode-cathode distance (mm)	4.5
- Anode wire dimension (mm)	0.02 x 130
- Cathode wire dimension (mm)	0.063 x 130
- Cathode group size	6.0
- Anode wire spacing (mm)	2.0
- Cathode wire spacing	0.55
- Grid transparency (ground)	90%
- Nominal HV (kV)*	
V_a, V_c, V_G	2.2, 0.5, 0

*Adjustable

REFERENCES

Anderson, D. F. 1981, Nucl. Instr. Methods, submitted.

Anderson, D. F., Ku, W. H.-M., Novick, R., and Scheckman, M. 1978, IEEE Trans. Nucl. Sci., **NS-15**, 813.

Andresen, R. D., Leimann, E. A., Peacock, A., and Taylor, B. G. 1977, Nucl. Instr. Methods, **146**.

Andresen, R. D., Leimann, E. A., Peacock, A., and Taylor, B. G. 1978, IEEE Trans. Nucl. Sci., **NS-25**, 800.

Charpak, G., Policarpo, A., and Sauli, F. 1980, IEEE Trans. Nucl. Sci., **NS-28**.

Conde, C. A. N., Ferreira, L. R., and Ferreira, F. A. 1977, IEEE Trans. Nucl. Sci., **NS-24**, 221.

Hamilton, T. T., Hailey, C. J., Ku, W. H.-M., and Novick, R. 1980, IEEE Trans. Nucl. Sci., **NS-27**, 190.

Hoan, N. N., Jeanjean, J., Itoh, H., and Charpak, G. 1980, Nucl.Instr. Methods, **172**, 603.

Ku, W. H.-M., and Hailey, C. J., 1981, IEEE Trans. Nucl. Sci., **NS-28**.

Ku, W. H.-M., Anderson, D. F., Hamilton, T. T., and Novick, R. 1979, IEEE Trans. Nucl. Sci., **NS-26**, 490.

Manzo, G., Peacock, A., Andresen, R. D., and Taylor, B. G. 1980, Nucl. Instr. Methods, **173**, 301.

Peacock, A., Andresen, R. D., Leimann, E. A., Long, A., Manzo, G., and Taylor, B. G. 1980, Nucl. Instr. Methods, **169**, 613.

Policarpo, A. J. P. L. 1978, Nucl. Instr. Methods, **153**, 389.

Reid, P. B., Ku, W. H.-M., Long, K. S., Novick, R., and Pisarski, R. L. 1979, IEEE Trans. Nucl. Sci., **NS-26**, 46.

FIGURE CAPTIONS

FIG. 1 - Schematic diagram of the imaging gas scintillation proportional counter (IGSPC).

FIG. 2 - Total pulse height from the cathode planes plotted as a function of anode high voltage (x); energy resolution plotted as a function anode high voltage (*). The data are for Cu-L with V_c = 0.5 kV and the GSPC at (3.8 - 0.5) kV.

FIG. 3 - The energy resolution vs.X-ray photon energy of the IGSPC. The solid line is proportinal to $E^{-1/2}$.

FIG. 4 - The energy (o) and position (•) resolution for Cu-L as a function of source position parallel to the anode wire direction.

FIG. 5- Position sensitivity and linearity in the direction parallel to the anode wires in the MWPC. The divider output is plotted vs. the source positon.

FIG. 6 - The IGSPC position resolution vs. X-ray photon energy. The solid line in proportional to $E^{-1/2}$.

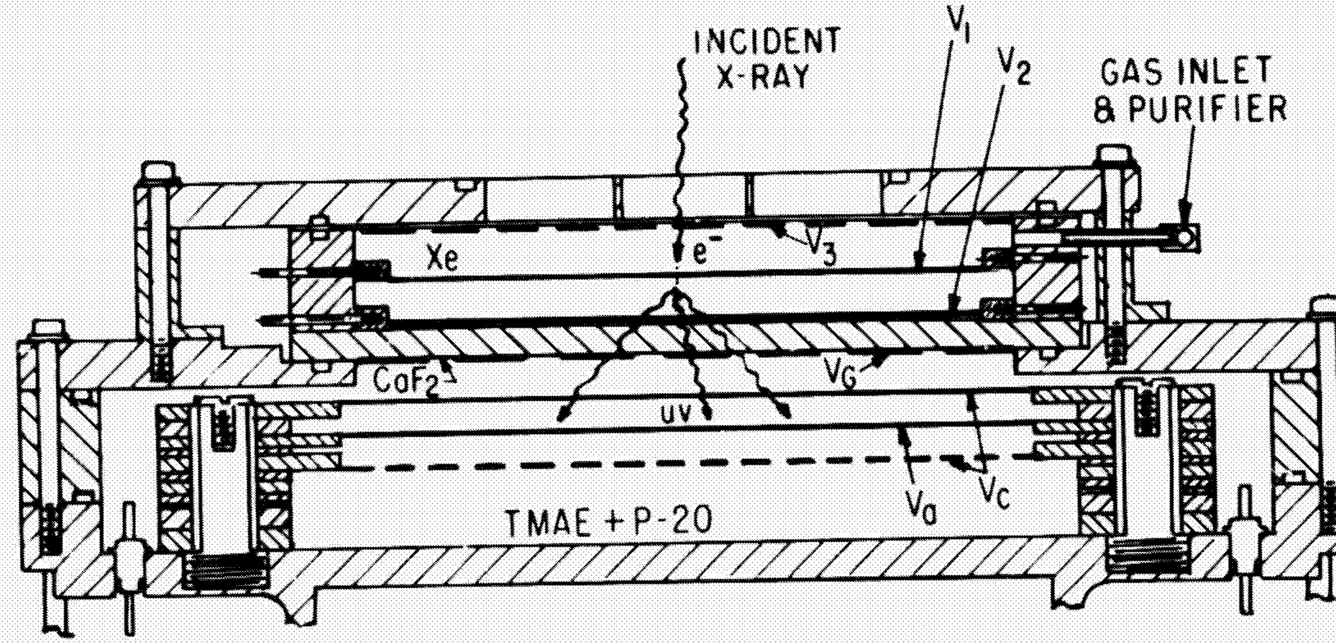
INCIDENT
X-RAY
V_1
V_2
GAS INLET
& PURIFIER
Xe
e^-
V_3
CaF_2
V_G
uv
V_a
V_c
TMAE + P-20

FIGURE 1

ORIGINAL PAGE IS
OF POOR QUALITY

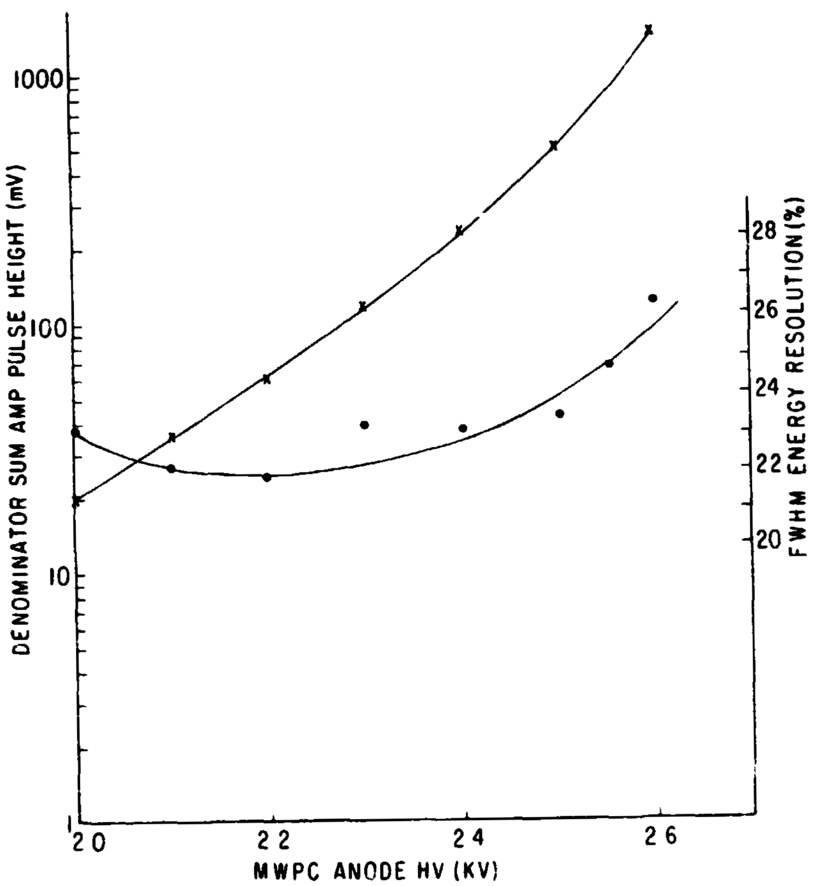

FIGURE 2

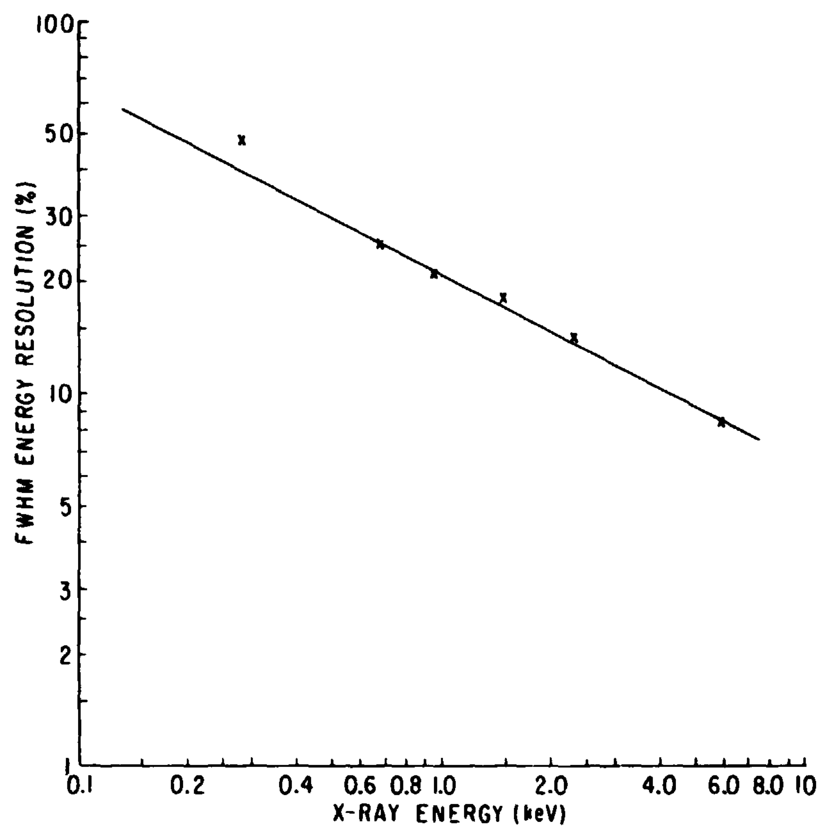
FWHM ENERGY RESOLUTION (%)
100
50
30
20
10
5
3
2
1
0.1
0.2
0.4
0.6
0.8
1.0
2.0
4.0
6.0
8.0
10
X-RAY ENERGY (keV)

FIGURE 3

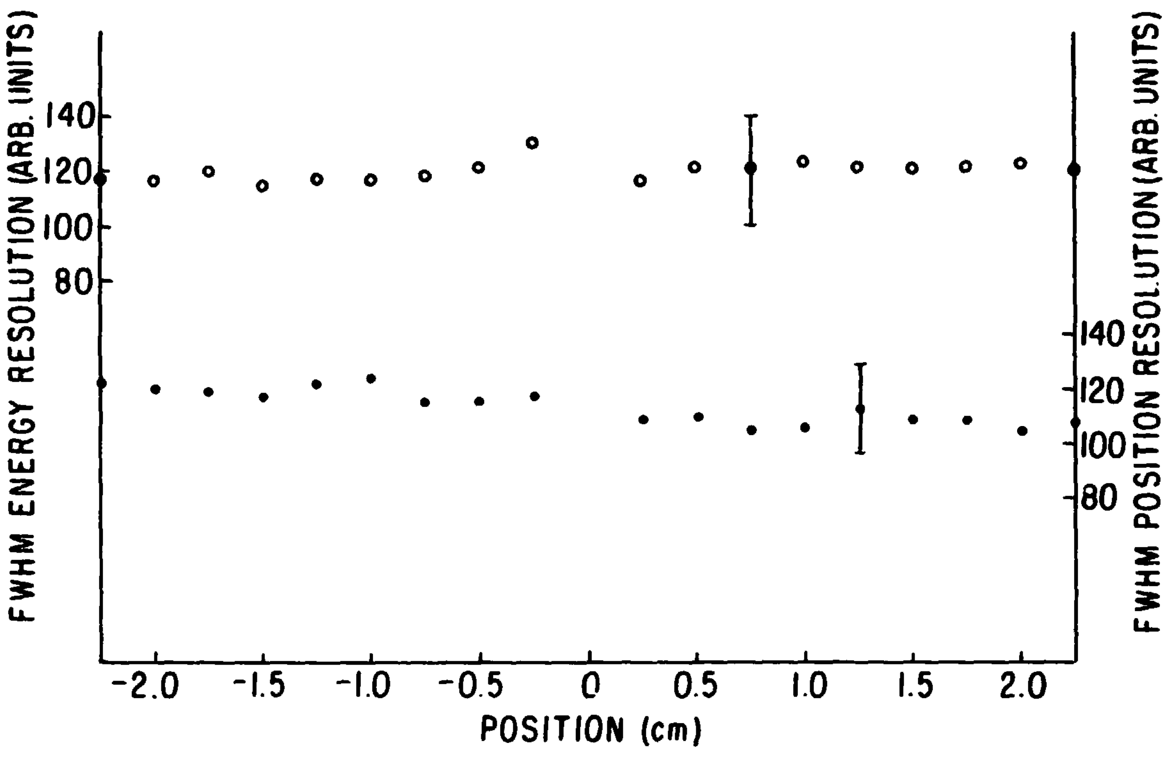
FWHM ENERGY RESOLUTION (ARB. UNITS)
140
120
100
80
FWHM POSITION RESOLUTION (ARB. UNITS)
140
120
100
80
-2.0
-1.5
-1.0
-0.5
0
0.5
1.0
1.5
2.0
POSITION (cm)

FIGURE 4

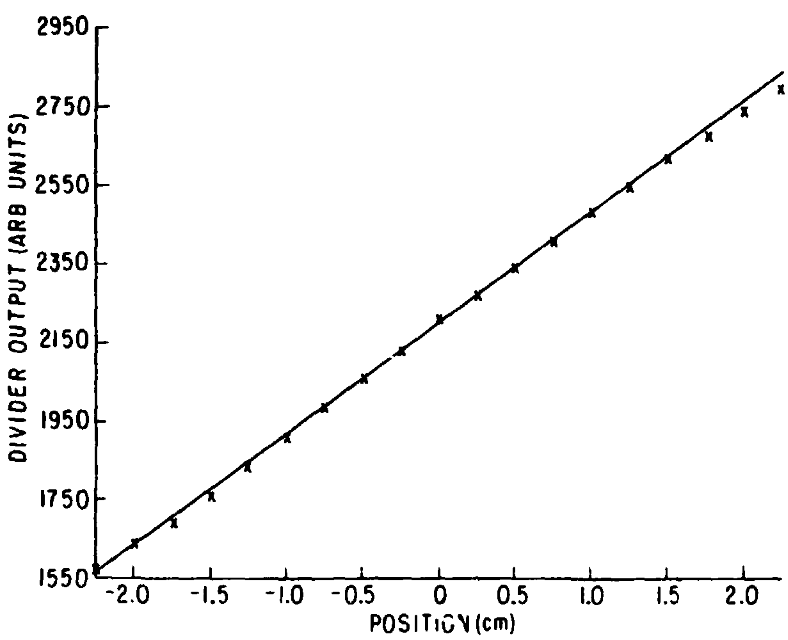
2950
2750
2550
2350
2150
1950
1750
1550
DIVIDER OUTPUT (ARB UNITS)
-2.0
-1.5
-1.0
-0.5
0
0.5
1.0
1.5
2.0
POSITION (cm)

FIGURE 5

ORIGINAL PAGE IS
OF POOR QUALITY

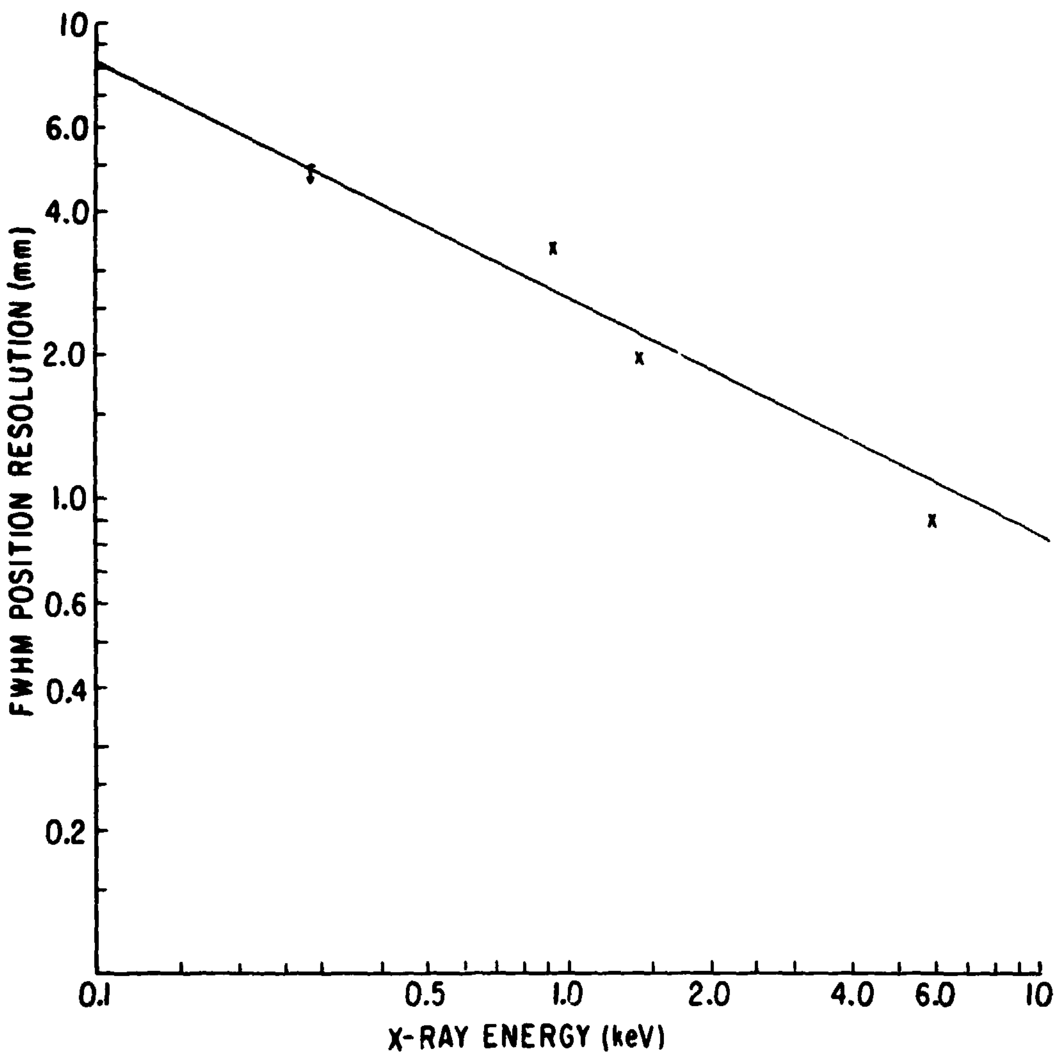

FIGURE 6